OPTICAL PROPERTIES OF CUBIC K_3Sb

V. A. Chaldyshev, V. P. Kiselev,
A. I. Klimin, and V. V. Konev

UDC 539.293.011

A number of optical characteristics of the crystal K_3Sb of cubic structure (the complex dielectric permeability function, the density of electron states, the refractive and absorptive indices, the optical density of the material) are computed on the basis of the electron energy spectrum calculated by the pseudopotential method taking account of nonlocality and spin—orbital interaction. Direct and indirect transition models to describe the optical excitation of electrons are discussed. Theoretical and experimental curves are compared.

Antimony alkaline compounds are used extensively in engineering as effective photocathodes. A sufficiently large quantity of experimental work devoted to the study of the optical and photoemission properties of these compounds has recently been executed. In this connection, there is the need for a theoretical investigation permitting an explanation of the experimental facts from a single viewpoint. Such an investigation cannot do without a study of the electron energy spectrum on whose basis information about the nature of the processes governing the optical and photoemission properties of the material can be obtained.

In previous papers [1-3], a theoretical study of the electron band structure and its associated optical properties was started for the antimony alkali compounds K_3Sb, KNa_2Sb, K_2CsSb, Na_3Sb, etc. A model of the effective Hamiltonian has been developed for this group of compounds in the approximation of rigid ions, taking account of the nonlocality and spin—orbit interaction. The fundamental qualitative features of the band structure of these compounds were set up.

Cubic K_3Sb, which is a characteristic and comparatively simple representative of this group of compounds, was selected as the object of a more detailed investigation in this paper. The band spectrum of K_3Sb was computed by the method of the pseudopotential, which was constructed in the form of a sum of ionic pseudopotentials V_K and V_{Sb} shielded by using the dielectric permittivity function $\varepsilon(q)$. The pseudopotential of potassium was selected in the form of a sum of local and nonlocal parts. The nonlocal part was given by the relationship

$$V_K^H(r) = \begin{cases} -A_2P_2, & r < R_K \\ 0, & r > R_K, \end{cases} \tag{1}$$

where P_2 is the projection operator on the subspace of functions convertible according to the representation of a rotation group with $l = 2$; $R_K = 2.51526$ atomic units is the core radius of potassium. The parameter A_2 was selected equal to 2.5958 Ry, as in [4]. The local part of the pseudopotential of the potassium ion and the pseudopotential of the antimony ion were given by the parametric formula

$$v(r) = \begin{cases} v_0\left(1 - \dfrac{r}{R_m}\right) - ze^2\left[\dfrac{r}{R_m^2} + c(r - R_m)r\right], & r \leqslant R_m \\ -\dfrac{ze^2}{r}, & r > R_m. \end{cases} \tag{2}$$

where v_0, R_m, and c are certain parameters and the form-factor of such a potential has the form

$$v(q) = \frac{4\pi ze^2}{\Omega q^2}\left(X(q) - \frac{X(q_0)\,Y(q)}{Y(q_0)}\right), \tag{3}$$

where

V. D. Kuznetsov Siberian Physicotechnical Institute at Tomsk State University. Translated from Izvestiya Vysshikh Uchebnykh Zavedenii, Fizika, No. 2, pp. 33-39, February, 1979. Original article submitted February 23, 1978; revision submitted April 12, 1978.

0038-5697/79/2202-0135$07.50

TABLE 1. Parameters of the Potassium and Antimony Ion Pseudopotential

Ion	Parameter				
	$\frac{q_0}{2\kappa_F}$	v_0 (Ry)	R_m (a.u.)	A_2 (Ry)	R_K
Potassium	0,92	2,2	3,8	−2,5958	2,51526
Antimony	0,835	−3,43	3,77	—	—

$\varepsilon_0 = 14{,}25$

$$X(q) = \left(\frac{v_0}{ze^2} + \frac{1}{R_m}\right)\left[\frac{2}{qR_m}(1 - \cos qR_m) - \sin qR_m\right] - \frac{1}{R_m}\sin qR_m;$$

$$Y(q) = \frac{2}{qR_m}(2\cos qR_m + 1) + \sin qR_m\left(1 - \frac{6}{(qR_m)^2}\right),$$

Ω is the volume of an elementary cell, q_0 is the first zero of the function v(q) (it is connected to the parameter c by the relationship $c = X(q_0)/R_m^2 Y(q_0)$). The function v(q) was cut off after the second zero in the computations.

In contrast to [1-3], a one-parameter function of the dielectric permittivity calculated by Green's function method in the Penn model [5] was used to describe the shielding:

$$\varepsilon(q) = 1 + \frac{4e^2\kappa_F m}{q^2\pi\hbar^2}\left\{1 + \frac{1}{\alpha}\left(-\operatorname{arsh}\alpha + \frac{1}{18}\operatorname{arsh}^3\alpha\right)\right\}, \tag{4}$$

where κ_F is the momentum of the free electron gas at the Fermi level, $\alpha = \kappa_F q\hbar^2/E_X m$; E_X is the energy gap approximately equal to the direct transition to the Brillouin zone at the point X, which is related to the value of the function $\varepsilon(q)$ at q = 0 by $\varepsilon(0) = 1 + (8\hbar^2e^2/9m)(\kappa_F^3/E_X^2)$. It is convenient to use the quantity $\varepsilon_0 = \varepsilon(0)$ as a parameter.

The pseudopotential parameters q_0, v_0, R_m of the antimony ion were selected by means of spectroscopic data from the correspondence between values of the fundamental optical transitions in a number of $A^{III}B^V$ compounds, including antimony, and experiment. The parameters of the local part of the potassium pseudopotential were selected so as to obtain the correct band structure for KCl. The value of the parameter ε_0 was selected from the considerations that the width of the K_3Sb forbidden band observed in test would be obtained. The values obtained for the parameters of the crystalline pseudopotential are presented in Table 1.

The spin–orbit interaction is taken into account in the model of Weisz [6], where the interaction parameter is selected such that the spin–orbit splitting at point Γ for K_3Sb agrees with Hübner's value $\Delta_{c.o}$=0.97 eV [7] for antimony alkali compounds.

The band structure of K_3Sb calculated with these parameters is presented in Fig. 1. The computation was performed by the κp-method in a regular mesh of Brillouin zone points. The spectrum structure and level symmetry at the points Γ, X, L, W of the K_3Sb Brillouin zone are the same as in [3]. Hence, in order not to clog the figure, the level symmetry is not shown. The characteristic features of the K_3Sb band structure are very flat valence bands, the presence of an optical gap between the first and second conduction bands, and also the sufficiently flat section in the first conduction band near the Brillouin zone boundary.

The density of the electron states (Fig. 1), defined by the formula

$$\rho(E) = \frac{2}{(2\pi)^3}\sum_i \int d^3\kappa\,\delta(E - E_i(\kappa)), \tag{5}$$

is calculated by using the Gilat–Raubenhaimer method [8]. There are three deltalike peaks on the curve $\rho(E)$ which describe the density of states in the flat valence bands. The density of states in the conduction band is small at first and then grows rapidly and oscillates around a certain mean value as the energy grows.

By using the Gilat–Raubenhaimer method, the frequency dependence of the imaginary part of the dielectric permittivity was also computed, which can be written in the form

$$\varepsilon_2(\omega) = \frac{e^2\hbar^2}{6m^2\omega^2\pi}\sum_{n,s}\int d^3\kappa\,|M_{ns}(\kappa)|^2\,\delta(E_n(\kappa) - E_s(\kappa) - \hbar\omega) \tag{6}$$

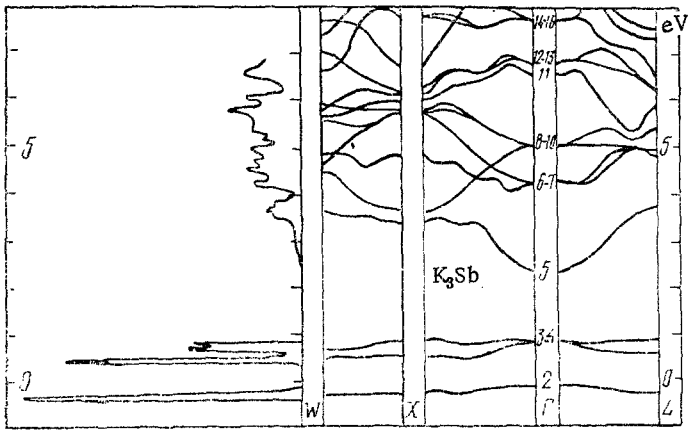

Fig. 1. Energy spectrum and the density of electron states.

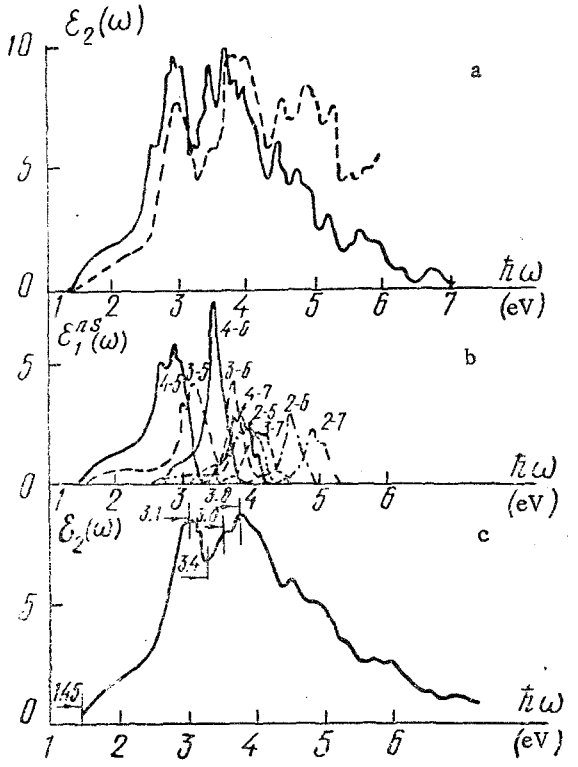

Fig. 2. Imaginary part of the dielectric permittivity ε_2 computed in the direct (solid line) and indirect (dashes) transition models without taking account of the effects of finiteness of the lifetime (a); contributions to ε_2 from direct transitions from the s-th (valence) band to the n-th (conduction) band (b); imaginary part of the dielectric permittivity in the direct transition model computed taking account of the finiteness of the lifetime (c).

in the dipole approximation in the direct transition model without taking account of the electron–phonon interaction. Here $M_{ns}(\kappa)$ are matrix elements of the optical transitions, $E_i(\kappa)$ is a function describing the dependence of the energy in the i-th band on the wave vector, and the summation over s is carried out in the valence band, while the summation over n is carried out in the conduction band (taking spin into account).

The dependence $\varepsilon_2(\omega)$ as well as the contributions of transitions from specific valence bands to the conduction bands (Fig. 2b) is shown in Fig. 2a. The numbering of the bands starts from the bottom so that the first conduction band is the fifth in this notation. It is seen that the first large peak on the curve $\varepsilon_2(\omega)$ is due to transitions from the third and fourth (valence) bands to the fifth (conduction) band. A comparison of the contributions from the different domains of the Brillouin zone showed that the principal contribution to

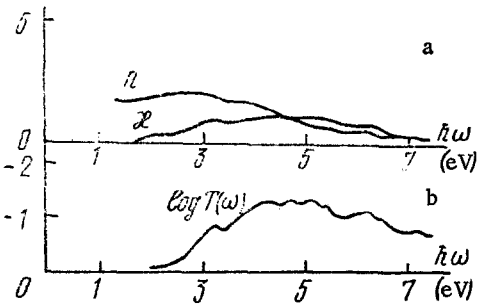

Fig. 3

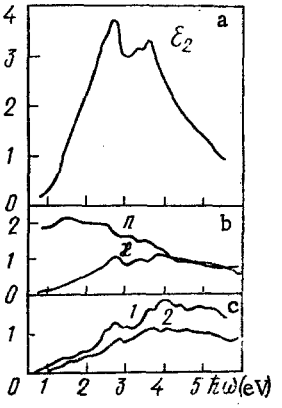

Fig. 4

Fig. 3. Theoretical curves of the refractive index n and the absorption index $\varkappa$(a); optical density of the substance log T computed for a film thickness d = 610 Å (b).

Fig. 4. Spectrum dependences of the imaginary part of the dielectric permittivity obtained experimentally [10] for cubic K_3Sb according to Sommer (a), refractive and absorptive indices (b), and optical density of the substance at d = 610 Å (c) for brown K_3Sb (curve 1) and cubic K_3Sb according to Sommer (curve 2).

the first peak is given by transitions from a sufficiently large volume in the neighborhood of the point X of the Brillouin zone. The valley between this and the next large peak is associated with the presence of the gap separating the fifth and sixth bands, and the peak is itself formed because of transitions from the fourth and third bands to the sixth and seventh, as well as of transitions from the second band (detached because of the spin–orbital interaction) to the fifth.

There is a foundation to assume [9] that the indirect transitions may make a substantial contribution to the optical excitation of electrons in K_3Sb. It can be shown that models of direct and indirect transitions yield similar results for compounds with narrow valence bands, as holds for K_3Sb. Indeed, by extracting the mean value of the matrix elements from under the integral sign in (6) and considering them independent of the energy, we obtain

$$\varepsilon_2(\omega) = \frac{e^2\hbar^2M^2}{6m^2\omega^2\pi}\sum_{n,s}\int dE'\int d^3\kappa\,\delta(E' - E_s(\kappa) - \hbar\omega)\,\delta(E' - E_n(\kappa)).$$

The E_s levels are almost independent of κ for the case of narrow valence bands so that the replacement of $\sum_s \delta(E' - E_s - \hbar\omega)$ by $\rho_v(E' - \hbar\omega)$ can be performed in the last integral (to the accuracy of a constant). Then taking account of (5), we arrive at the expression

$$\varepsilon_2(\omega) \sim \int \rho_c(E')\,\rho_v(E' - \hbar\omega)\,dE', \qquad (7)$$

which is obtained in the indirect transition model (ρ_c is the density of the states in the conduction band and ρ_v in the valence band).

Curves for $\varepsilon_2(\omega)$ calculated by means of (6) and (7) are presented in Fig. 2a. It is seen that the curves have identical singularities but the curve corresponding to the indirect transitions model (dashes) drops more slowly as ω grows. This circumstance is apparently associated with the fact that the dependence of the transition probability on the energy is not taken into account in (7).

A frequency dependence $\varepsilon_2(\omega)$ (Fig. 4a) with a sufficiently rapid drop in the area of large ω is obtained from experimental results in [10], which apparently indicates a diminution in the transition probability with the rise in the transition energy.

There is a large quantity of singularities missing from the experimental curve in the $\varepsilon_2(\omega)$ curves (Fig. 2a). This circumstance is associated both with the imperfection in the

experiment technique (limited resolution of the instruments, disorder in the real structure of K_3Sb) and with not taking account of the different electron-scattering effects. All these factors can be taken into account phenomenologically by introducing the effective spectral line broadening by replacing the delta function $\delta(x)$ in (6) by a certain deltalike function $L(x)$. We selected $L(x)$ in the form

$$L(x) = \frac{1}{\pi} \frac{\Gamma}{\Gamma^2 + x^2}$$

and took the broadening parameter Γ equal to 0.005 Ry.

The curve $\varepsilon_2(\omega)$ obtained is presented in Fig. 2c. On the whole, its configuration agrees with the configuration of the experimental curve (Fig. 4a). However, the location of the singularities on the theoretical curve is shifted somewhat toward the higher photon energy domain. The spacing between the two main peaks is 0.7 eV on the theoretical dependence $\varepsilon_2(\omega)$, which is in satisfactory agreement with the experimental value of 0.9 eV. On the whole, the computed curve $\varepsilon_2(\omega)$ is above the experimental curve. Thus, the theoretical value in the first peak is approximately twice the experimental value. This is apparently related to the fact that the matrix elements of the optical transitions M_{ns} were evaluated by means of pseudo-wave functions. In conformity with this, it is expedient to normalize $\varepsilon_2(\omega)$ so that the theoretical and experimental values at the first peak would agree. By knowing the spectral dependence $\varepsilon_2(\omega)$, the real part of the dielectric permittivity can be reproduced by the Kramers—Kronig relationship. The "tail" of ε_2 was approximated by a two-parameter rational fraction. The parameters were selected from the conditions of continuity of the function ε_2 and its derivative at the merger point. The refractive n and absorptive $\varkappa$ indices were computed by means of the calculated dependencies $\varepsilon_1(\omega)$ and $\varepsilon_2(\omega)$. Their graphs are presented in Fig. 3a.

The theoretical dependencies $n(\omega)$ and $\varkappa(\omega)$ agree with the experimental data for cubic K_3Sb [10] (Fig. 4b). The 3.7-5.5-eV domain on the computed curve $\varkappa(\omega)$ is a domain of strong optical absorption ($\varkappa \geq 1$). As the photon energy grows, the absorptive index $\varkappa$ slowly decreases. The refractive index n has only a weak dependence on ω on both the theoretical and experimental curves for low photon energies. This dependence becomes substantial only in the domain $\hbar\omega > 2.5$ eV. On the curve $n(\omega)$ there is a valley at $\hbar\omega \approx 3.3$ eV and a stable drop in the energy domain to 5.5 eV.

It is of known interest to compare the results obtained theoretically with the characteristics measured directly. To this end, we computed the spectral dependence of the coefficient of optical passage T through a layer of substance of thickness 610 Å for cubic K_3Sb (Fig. 3b).

A detailed comparison of the theoretical curves with experiment is made complicated by the fact that quantitative information about the optical characteristics communicated by different authors, differ noticeably. Thus, the dependencies $\log T(\omega)$ for brown K_3Sb and cubic K_3Sb according to Sommer behave substantially distinctly (Fig. 4c). Although the positions of the main peaks agree (one peak at $\hbar\omega = 2.75$ eV and a double peak at $\hbar\omega = 3.65$; 3.9 eV), there is, however, not the quite definite minimum at $\hbar\omega = 3.25$ eV for brown K_3Sb on the curve of cubic K_3Sb according to Sommer. These differences are related to the distinct technologies used to obtain the K_3Sb films.

The configuration of the theoretical curve $\log T(\omega)$ (Fig. 3b) agrees on the whole with the configuration of the experimental dependence for cubic K_3Sb according to Sommer. However, the singularities on the curve considered are shifted somewhat toward high values of the photon energy relative to the experimental curves. We have already noted such a shift in discussing the spectral dependence $\varepsilon_2(\omega)$. The band spectrum model proposed therefore permits an explanation of the fundamental configurational singularities in the optical characteristics of cubic K_3Sb.

LITERATURE CITED

1. A. A. Mostovskii, V. A. Chaldyshev, G. F. Karavaev, A. I. Klimin, and I. N. Ponomarenko, Izv. Akad. Nauk SSSR, Ser. Fiz., 38, 195 (1974).
2. V. A. Chaldyshev, V. P. Kiselev, and N. A. Zakharov, in: Chemical Coupling in Crystals and Their Physical Properties [in Russian], Vol. 2, Nauka i Tekhnika, Minsk (1976).
3. A. A. Mostovskii, V. A. Chaldyshev, V. P. Kiselev, and A. I. Klimin, Izv. Akad. Nauk SSSR, Ser. Fiz., 40, 2490 (1976).

4. M. J. G. Lee and L. M. Falicov, Proc. R. Soc., A304, 319 (1968).
5. V. G. Tyuterev, Izv. Vyssh. Uchebn. Zaved., Fiz., No. 3, 152 (1974).
6. G. Weisz, Phys. Rev., 149, 504 (1966).
7. K. Hübner, Ann. Phys., 25, 97 (1970).
8. G. Gilat and L. J. Raubenhaimer, Phys. Rev., 144, 390 (1966).
9. W. E. Spicer and R. K. Iden, Proceedings of the Ninth International Conference on Semiconductor Physics [in Russian], Vol. 1, Nauka, Moscow (1969).
10. A. Ebina and T. Takahasi, Phys. Rev., B7, 4712 (1973).

SPIN EQUATIONS OF MOTION IN AN EXTERNAL FIELD. II

I. M. Ternov, V. R. Khalilov,
and O. S. Pavlova

UDC 530.145

In [1] the derivation of chemical equations of motion for the electron spin by rigorous quantum-mechanical methods was considered. In contrast to a number of well-known works [2-4], accurate quantum-mechanical equations of motion which were functionally the same as the corresponding classical equations of motion were obtained for the even components of the spin operators. Thus, in this case, the transition to classical equations is made simply by replacing the even components of the operators by their quantum-mechanical mean over the given state.

Note further that all the conditions imposed in the previous approaches [2-4] on the freedom of choice of the wave packet over which the equations of motion are averaged are satisfied automatically in the present approach, in which, in fact, all the operator equations of motion were constructed within the framework of single-particle theory. In addition, the description of a quantum system using the even components of the operators alone is only possible under the condition that the motion is quasiclassical.

1. Conditions of Applicability of Classical Equations of Motion of Electron Spin

Thus, the conditions of applicability of the spin equations of motion obtained in the present approach [1, 3] may be formulated as follows.

a) The particle wave function must be a packet of width $a > \hbar/mc$ that is localized close to the classical trajectory (in the intrinsic reference system).

b) The particle momentum must not vary greatly over distances of the order of the wavelength $\hbar/|p|$ and at distances of order $\hbar/a$ (condition of quasiclassical motion).

c) The electromagnetic field in which the electron is moving must be sufficiently small in the quasiclassical sense. For example, for particle motion in a magnetic field, the radius of the quasiclassical orbit may be taken as the characteristic length L:

$$L = R = \sqrt{\frac{n+1/2}{\gamma}} = \frac{cp}{eH}$$

[5]. Then the condition of quasiclassical motion requires that $R \gg \hbar/mc$ or $e\hbar H/mpc^2 \ll 1$. Introducing the characteristic parameter $\chi = (H/H_{cr})(p/mc)$, where $H_{cr} = m^2c^3/e\hbar$, this condition may be rewritten in the form

$$\chi\left(\frac{mc}{p}\right)^2 \ll 1.$$

At small particle momenta (nonrelativistic approximation), the condition of applicability of the resulting equations of motion transforms to the requirement $H < H_{cr}$. A stronger constraint derives from the requirement of sufficiently smooth change in the field at distances of the order of the packet width:

M. V. Lomonosov Moscow State University. Translated from Izvestiya Vysshikh Uchebnykh Zavedenii, Fizika, No. 2, pp. 39-44, February, 1979. Original article submitted January 17, 1978.

 0038-5697/79/2202-0140$07.50